AGU ADVANCING EARTH AND SPACE SCIENCE

Geophysical Research Letters

RESEARCH LETTER
10.1029/2020GL091733

Surface Melt and Runoff on Antarctic Ice Shelves at 1.5°C, 2°C, and 4°C of Future Warming

E. Gilbert[1,3] **and C. Kittel**[2]

[1]British Antarctic Survey, Cambridge, UK, [2]Department of Geography, Laboratory of Climatology, SPHERES, University of Liège, Liège, Belgium, [3]Now at Department of Meteorology, University of Reading, Reading, UK

Key Points:

- More sustained atmospheric warming leads to elevated melt and runoff, which may suggest ice shelf destabilization
- 34% of Antarctic ice shelf area could be vulnerable to collapse at 4°C of warming above pre-industrial levels
- The Larsen C, Wilkins, Pine Island, and Shackleton ice shelves are identified using projected melt and runoff to be most susceptible

Supporting Information:

Supporting Information may be found in the online version of this article.

Correspondence to:

E. Gilbert,
ella.gilbert@reading.ac.uk

Citation:

Gilbert, E., & Kittel, C. (2021). Surface melt and runoff on Antarctic ice shelves at 1.5°C, 2°C, and 4°C of future warming. *Geophysical Research Letters*, *48*, e2020GL091733. https://doi.org/10.1029/2020GL091733

Received 20 NOV 2020
Accepted 25 MAR 2021

Abstract The future surface mass balance (SMB) of Antarctic ice shelves has not been constrained with models of sufficient resolution and complexity. Here, we force the high-resolution Modèle Atmosphérique Régional with future simulations from four CMIP models to evaluate the likely effects on the SMB of warming of 1.5°C, 2°C, and 4°C above pre-industrial temperatures. We find non-linear growth in melt and runoff which causes SMB to become less positive with more pronounced warming. Consequently, Antarctic ice shelves may be more likely to contribute indirectly to sea level rise via hydrofracturing-induced collapse, which facilitates accelerated glacial discharge. Using runoff and melt as indicators of ice shelf stability, we find that several Antarctic ice shelves (Larsen C, Wilkins, Pine Island, and Shackleton) are vulnerable to disintegration at 4°C. Limiting 21st century warming to 2°C will halve the ice shelf area susceptible to hydrofracturing-induced collapse compared to 4°C.

Plain Language Summary Whether Antarctic ice shelves are gaining or losing ice at the surface—their surface mass balance (SMB)—depends on many factors. To understand future Antarctic ice shelf SMB requires complex computer models, and until now, few studies using these models have been done. Here, we use the high-resolution MAR model to explore how ice shelf SMB changes under warming scenarios of 1.5°C, 2°C, and 4°C above pre-industrial temperatures. Our results show that warming causes SMB to decrease because high temperatures produce meltwater, which then runs off the ice shelves, and that this effect is larger for greater levels of warming. Antarctic ice shelves may contribute to rising sea levels in future because larger amounts of melt and runoff increase their vulnerability to "hydrofracturing," a process whereby ice shelves crack and disintegrate. Limiting future warming will reduce the number of ice shelves that will be susceptible to collapse via this mechanism.

1. Introduction

The collapse, thinning, or recession of Antarctic ice shelves influences sea level rise by reducing shelf buttressing and allowing tributary glaciers to accelerate, increasing ice discharge into the ocean (Borstad, 2013; Fürst et al., 2016; Lai et al., 2020; Rignot et al., 2004; Trusel et al., 2015). Atmospheric and oceanic processes have driven recent thinning of Antarctic ice shelves, causing mass loss from the Antarctic ice sheet (Gudmundsson et al., 2019; Paolo et al., 2015; Pritchard et al., 2012). Although present mass loss from Antarctic ice shelves is primarily related to ice and ocean dynamical changes caused by iceberg calving and basal melting, respectively (Shepherd et al., 2018), surface processes such as melt are useful indicators of ice shelf stability and hence their likely contribution to sea level rise because of the importance of surface processes in driving ice shelf fracture and collapse (Bell et al., 2018; Kingslake et al., 2017). The role of surface processes can be summarized in the surface mass balance (SMB), the difference between accumulation and ablation processes.

Hydrofracturing-induced ice shelf collapse is triggered by prolonged surface melt and densification of the buffering firn layer. Repeated seasons where meltwater production exceeds new firn formation drives saturation of the firn layer, meaning new meltwater collects on the surface and fills existing rifts and crevasses. Crevasses widen at the tip through the hydrostatic pressure of water (Kuipers Munneke et al., 2014). Ice shelves saturated with refrozen meltwater are susceptible to collapse, such as occurred on the Antarctic Peninsula (Kuipers Munneke et al., 2018; Scambos et al., 2000, 2003; van den Broeke, 2005). This means runoff can be used as an indicator of shelf stability because runoff occurs only when meltwater cannot refreeze in the snowpack, implying that hydrofracturing is possible. A recent study (Lai et al., 2020) evaluates

the dynamical stress regimes of Antarctic ice shelves to identify those that are vulnerable to collapse via this mechanism, motivating the focus on surface processes.

As atmospheric warming continues, changes in precipitation, melt and runoff will cause ice shelf SMB to evolve and may increase their indirect contribution to sea level (Lhermitte et al., 2020). However, future ice shelf melt, runoff and SMB are associated with large uncertainties (Lenearts et al., 2019; Ligtenberg et al., 2013; Trusel et al., 2015).

The use of high-resolution regional models (RCMs, grid spacing of ~10s of km) is necessary to resolve the boundary layer processes and interactions that drive SMB, such as topography, precipitation and sublimation (Favier et al., 2017; Lenaerts et al., 2019). While several studies have used the latest RCMs to evaluate present-day SMB (e.g., Agosta et al., 2019; Mottram et al., 2021; Souverijns et al., 2019; van Wessem et al., 2018), most analyses of future SMB have been conducted using coarse-resolution global climate models (GCMs, grid-spacing of ~100s km) or older generation RCMs which perform more poorly with respect to SMB and melt (e.g., Lenaerts et al., 2016; Ligtenberg et al., 2013). This study improves upon these by using the latest generation of the Modèle Atmosphérique Régional (MAR), which includes more sophisticated parameterizations of processes like sublimation and cloud microphysics, to downscale GCM projections to higher resolution.

Ice shelf surface melting and runoff is projected to increase with warming (Kittel et al., 2021; Trusel et al., 2015). However, the relationship between temperature and melting is highly non-linear, and melt rates associated with different future scenarios diverge considerably around mid-century, resulting in a wide range of values for 2100 (Trusel et al., 2015). It is therefore justifiable to examine SMB under various increments of global mean warming, rather than comparing models that simulate a wide range of temperature anomalies in 2100. Kittel et al. (2021) use this approach in their analysis of the future Antarctic ice sheet SMB using MAR. They show that the threshold above which runoff anomalies exceed precipitation anomalies over ice shelves (causing SMB to become negative) is around 2°C, after which point melt and runoff totals of this magnitude could trigger ice shelf speedup, shearing and further damage that could weaken shelves in a positive feedback (Lhermitte et al., 2020). Constraining the response of Antarctic ice shelves under warming scenarios of 1.5°C, 2°C, and 4°C will therefore improve understanding of the likely impact of future warming on Antarctic mass loss and sea level rise.

2. Materials and Methods

MAR is a hydrostatic RCM adapted to study the polar regions (Gallée & Schayes, 1994), with sophisticated cloud microphysics (Gallée, 1995; Gallée & Gorodetskaya, 2010). The snow surface scheme (Gallée & Duynkerke, 1997; Gallée et al., 2001) includes prognostic equations for water content, temperature, mass, and snow properties. It also simulates the evolution of snow albedo (see Tedesco et al., 2016), meltwater percolation and retention in the snowpack. When snowpack water content exceeds 5%, the remaining liquid, which may originate from rainfall or meltwater, is converted to runoff. Without a liquid-water routing scheme to simulate melt ponding, runoff is removed from the snowpack and assumed to flow directly into the ocean. Runoff therefore indicates the presence of liquid water at the surface. For further details of the model setup see Kittel et al. (2021). MAR is run at an intermediate grid spacing of 35 km: A compromise between computational efficiency and resolution. Although at 35 km MAR smoothes complex topography, for example on the Antarctic Peninsula, it adequately resolves near-surface climate and melt over the historical period (Mottram et al., 2021). Validation of MAR's performance relative to observed SMB and near-surface climate is presented in Mottram et al. (2021) and the four MAR simulations are evaluated in Kittel et al. (2021). For this reason, the historical period is not considered further.

GCM simulations of the period 1980–2100 using ACCESS1.3 and NorESM1-M (CMIP5 models), and CESM2 and CNRM-CM6-1 (CMIP6) under RCP8.5 (ACCESS1.3 and NorESM1-M) and ssp585 (CESM2 and CNRM-CM6-1) are dynamically downscaled using MAR. GCMs are selected based on the availability of 6-h outputs, the diversity of warming scenarios they provide, and their ability to represent current Antarctic climate as determined by Agosta et al. (2015). For further detail of the model selection criteria, see Section S1.1 of the supporting information.

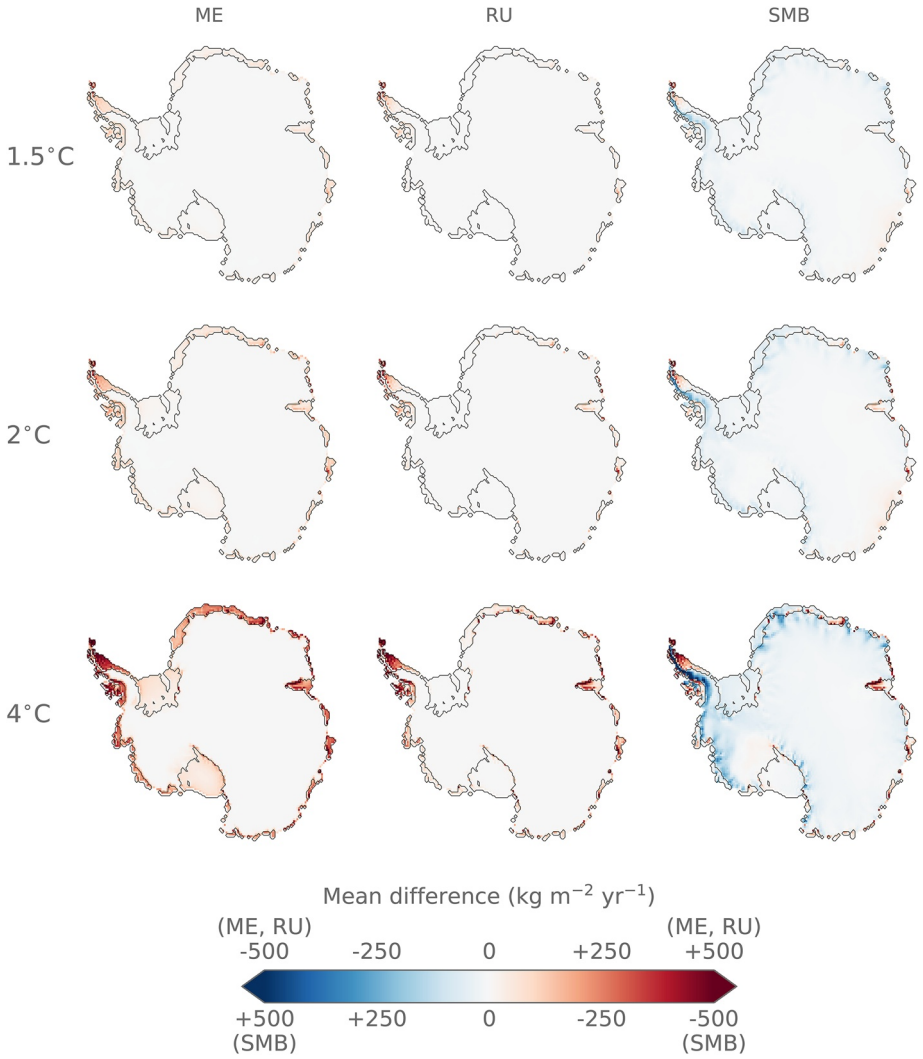

Figure 1. Multi-model mean melt (ME), runoff (RU), and surface mass balance (SMB) under the 1.5°C, 2°C, and 4°C warming scenarios, expressed as the difference relative to the historical period, 1980–2009. Warm and cool colors indicate an increase and decrease relative to the historical period, respectively, for melt and runoff, while the color scale is reversed for SMB.

Because the forcing GCMs simulate different pre-industrial temperatures (defined as the mean of global mean modeled near-surface air temperature between 1850-1879) and some exhibit much larger warming by 2100 than others (cf. Agosta et al., 2015; Kittel et al., 2021), scenarios are considered in which global mean temperature increase is equal to 1.5°C, 2°C, and 4°C above pre-industrial. This method allows us to focus on the effect of warming on the SMB and prevents GCMs with greater end-of-century warming having a larger influence on the MAR projections, thereby reducing model uncertainty, a first-order source of uncertainty in temperature and precipitation projections, and hence the projected SMB (Hawkins & Sutton, 2011). For each GCM and the multi-model mean (MMM), the 30-year periods where warming reaches these intervals are identified by subtracting the 30-years running mean near-surface temperature from the pre-industrial temperature. Consequently, the periods in which warming is equal to 1.5°C, 2°C, and 4°C are different in each model.

2.1. The Effect of Future Warming on Surface Mass Balance Components

Figure 1 shows changes in MMM melt, runoff and SMB at 1.5°C, 2°C, and 4°C above pre-industrial temperatures relative to the historical period 1980–2009. Increases in melt and runoff are concentrated over

Table 1
Mean Modeled Values of Melt (ME), Runoff (RU), and Surface Mass Balance (SMB), in Gt yr^{-1}, Over Antarctic Ice Shelves Simulated by MAR Forced With Each GCM Under the Historical (1980–2009), 1.5°C, 2°C, and 4°C Global Mean Surface Warming Scenarios

Ariable	Forcing model	Historical mean	1.5°C	2°C	4°C
ME	ACCESS1.3	122.8	161.6	210.0	362.6
	CESM2	79.8	115.7	138.0	394.2
	NorESM1-M	73.0	96.4	118.4	254.9
	CNRM-CM6-1	92.2	166.7	232.9	494.3
	MMM	**91.9**	**135.1**	**174.8**	**376.5**
RU	ACCESS1.3	41.5	58.1	78.3	166.9
	CESM2	16.5	29.2	41.7	176.8
	NorESM1-M	15.7	22.9	32.8	89.1
	CNRM-CM6-1	17.5	53.0	81.1	253.0
	MMM	**22.8**	**40.8**	**58.5**	**171.5**
SMB	ACCESS1.3	440.7	447.2	445.3	384.3
	CESM2	473.4	485.4	488.2	432.1
	NorESM1-M	525.9	537.6	531.9	543.6
	CNRM-CM6-1	488.0	490.7	475.3	371.0
	MMM	**482.0**	**490.2**	**485.2**	**432.7**

Note. The multi-model mean (MMM) for each variable under each scenario is highlighted in bold.
GCM, global climate models; MAR, Modèle Atmosphérique Régional.

ice shelves while positive and negative SMB changes are simulated over grounded ice and ice shelves, respectively. Table 1 shows annual mean values of melt, runoff and SMB on ice shelves during the historical period and under each future warming scenario for all models. At greater levels of warming, especially at 4°C, melt and runoff increase considerably, causing ice shelf SMB to become more negative (Table 1, Figure 1). Elevated runoff totals indicate that ice shelves become increasingly saturated with refrozen meltwater and rainfall and suggest conditions conducive to hydrofracturing. This picture differs from that over grounded ice, where SMB tends to increase due to enhanced precipitation, especially over the steep terrain of the Antarctic periphery and trans-Antarctic mountains (Figure 1). Further detail of precipitation changes is given in Section S2.1.

The four models simulate comparable ice shelf melt, runoff, and SMB values for the historical period: ACCESS1.3 simulates the highest melt and runoff and the lowest SMB (129 Gt yr^{-1}, 42 Gt yr^{-1}, and 441 Gt yr^{-1}, respectively), while the lowest melt and runoff and highest SMB are simulated by NorESM1-M (73 Gt yr^{-1}, 16 Gt yr^{-1}, and 526 Gt yr^{-1}, respectively; Table 1). As shown in Table 1 and Figure 2, the inter-model spread in these variables increases with warming, for example SMB rises from ±43 Gt yr^{-1} (±9%) of the MMM in the historical period to ±86 Gt yr^{-1} (±20%) at 4°C, reflecting greater model uncertainty at longer lead times. NorESM1-M consistently simulates the highest SMB and lowest melt and runoff values at all warming intervals. However, the models broadly agree, showing increased ice shelf melt and runoff with greater warming and a consequent decline in SMB. Further, the sensitivity of melt to warming compares well with the sensitivity found by Trusel et al. (2015) (see Section S2.2, Figure S6), suggesting that these findings are robust.

Table 1 and Figure 2 show limited differences in mean melt, runoff and SMB between the 1.5°C and 2°C scenarios, but that considerable changes are simulated at 4°C relative to the historical period. This may indicate a non-linear response of the SMB to warming, also shown by Kittel et al. (2021), whereby modest warming of 1.5°C or 2°C causes ice shelves to gain mass as precipitation inputs increase more rapidly than melt or runoff, but that more sustained warming of 4°C or more is associated with a declining SMB as the magnitude of increases in melt and runoff begins to exceed the growth in precipitation rates. Table 1 shows that warming of 4°C leads to considerable increases in MMM melt (+241 Gt yr^{-1}) and runoff (+131 Gt yr^{-1}) compared to the 1.5°C scenario. In three out of four models this causes SMB to decline, but NorESM1-M simulates a + 6 Gt yr^{-1} increase in SMB in the 4°C scenario compared to the 1.5°C scenario due to increased precipitation (Table 1, Figures S1 and S2).

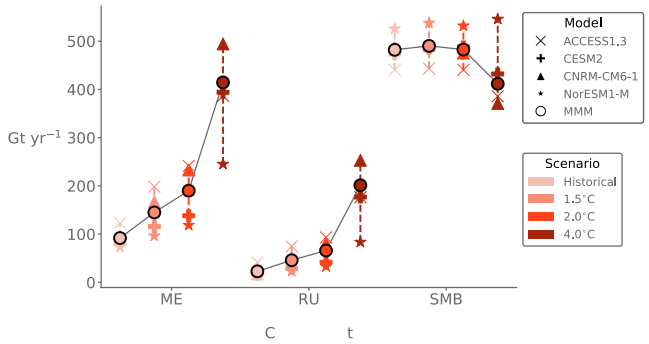

Figure 2. Plot showing mean total melt (ME), runoff (RU) and surface mass balance (SMB), in Gt yr^{-1}, for Antarctic ice shelves during the historical period (1980–2009) and for global mean warming scenarios of 1.5°C, 2°C, and 4°C above pre-industrial levels in all GCM-forced MAR simulations. Colors indicate the scenario, and each model is plotted with a unique marker. The MMM is indicated with outlined circle and dashed vertical lines indicate the inter-model spread. GCM, global climate models; MAR, Modèle Atmosphérique Régional; MMM, multi-model mean.

2.2. Ice Shelf Runoff Extent and Duration

Annual runoff totals can indicate ice shelf stability because the presence of liquid water on the surface implies a snowpack saturated with refrozen meltwater and rainfall and suggests that hydrofracturing-induced shelf disintegrations could be possible. Figure 3 shows time series of the percentage of ice shelf area where runoff occurs in each sector of Antarctica. A comparable figure showing melt extent above the snowfall-adjusted threshold of Pfeffer et al. (1991) indicative of destabilization is given in the supplement (Figure S7, Section S2.3). Figure 4 shows the mean

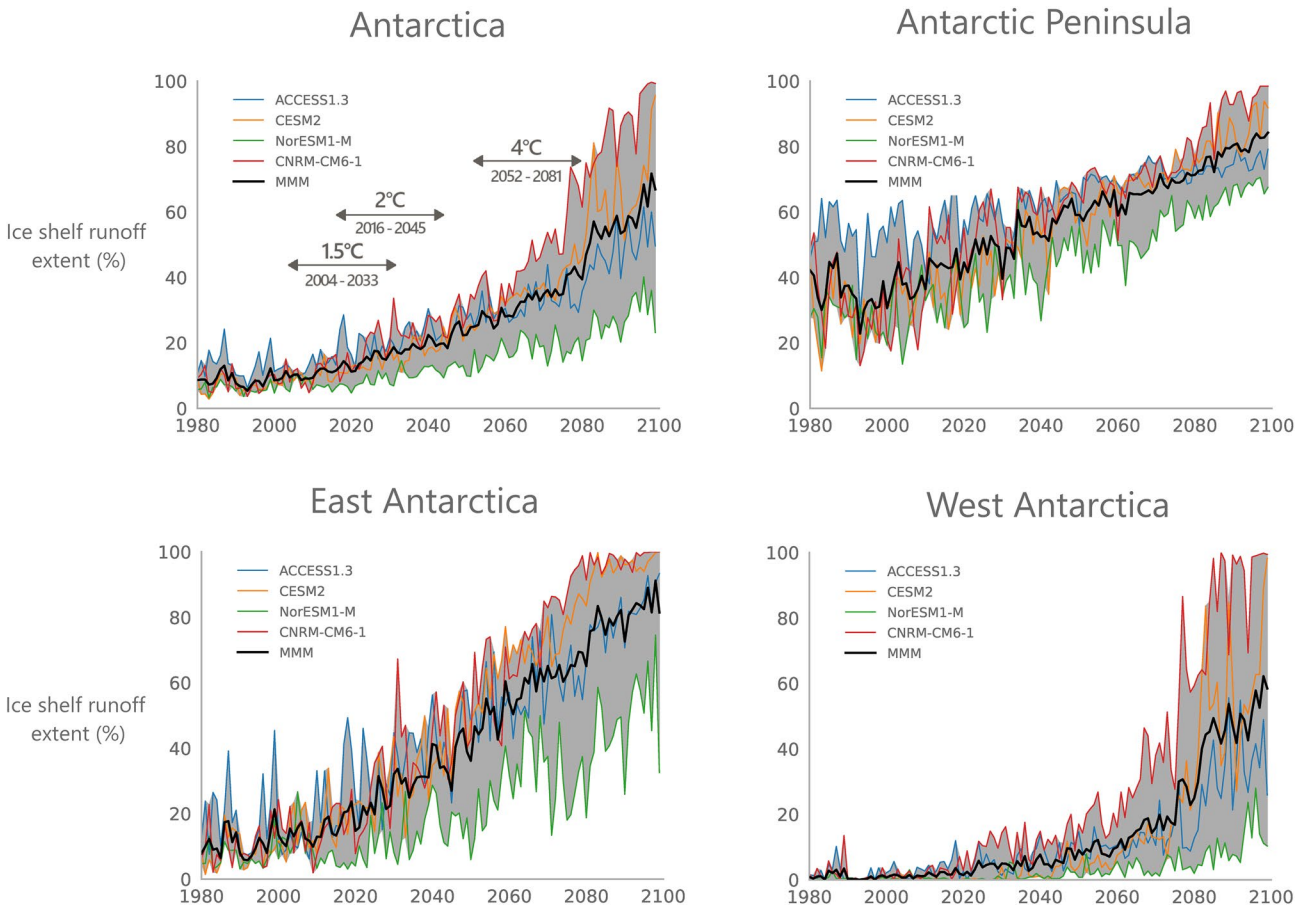

Figure 3. Mean simulated ice shelf extent, expressed as a percentage of total area, where runoff is simulated in various sectors of the Antarctic (Antarctic Peninsula, East Antarctica, and West Antarctica) and the entire continent (Antarctica) throughout the 21st century. Individual model simulations are indicated with colored lines, while the multi-model mean (MMM) is shown with the solid black line and the shaded region shows the inter-model spread. The time periods during which MMM warming of 1.5°C, 2°C, and 4°C above pre-industrial temperatures is simulated are indicated in the upper left panel.

number of days per year under each scenario where daily mean ice shelf runoff of at least 1 kg m^{-2} d^{-1} is projected in each simulation, plus the MMM runoff duration at 4°C.

In all sectors, the portion of total ice shelf area where runoff is simulated increases with warming—from 14% (8.5%–19.9%) at 1.5°C to 34% (22.6%–42.9%) at 4°C—however, this varies spatially. Simulated runoff extent and duration is largest on the Antarctic Peninsula during all time intervals—at 1.5°C, liquid water is present at the surface on 46% (37.5%–59.1%, Figure 3) of the peninsula's ice shelves and occurs on average for 13 d yr^{-1} (8–19 d yr^{-1}), with runoff concentrated in the northwestern extremities of the Larsen C ice shelf (Figures 4 and S8). However, at 4°C, the region expands to cover a greater extent of Larsen C, plus the Wilkins and George VI ice shelves (ACCESS1.3 and CNRM-CM6-1, Figures 4 and S8), a total area of 66.8% (60.8%–71.4%, Figure 3), and runoff duration increases on average to 36 d yr^{-1} (23–39 d yr^{-1}, Figure 4). At 4°C the MMM runoff duration is highest on the northwestern tip of the peninsula, where liquid water is present at the surface during 143 d yr^{-1}, with surface water present for up to 93, 81, and 75 d yr^{-1} on the Larsen C, Wilkins and George VI ice shelves, respectively (Figure 4).

Meanwhile, surface liquid water is present over a limited part of West Antarctica, even at 4°C (17.5%, 6.6%–29.6%, Figure 3), with the highest values simulated near the inner peripheries of the Abbot, Cosgrove and Pine Island ice shelves, a result also found by Donat-Magnin et al. (2021). This may be because snowfall increases offset increased melt rates (Figure S1). Only the CNRM-CM6-1 simulation produces runoff over other ice shelves in the Amundsen Sea embayment (Figures 4 and S8). Across all West Antarctic ice shelves, runoff is simulated infrequently in all scenarios, rising from on average 1 d yr^{-1} (0–1 d yr^{-1}) at 1.5°C to 4 d

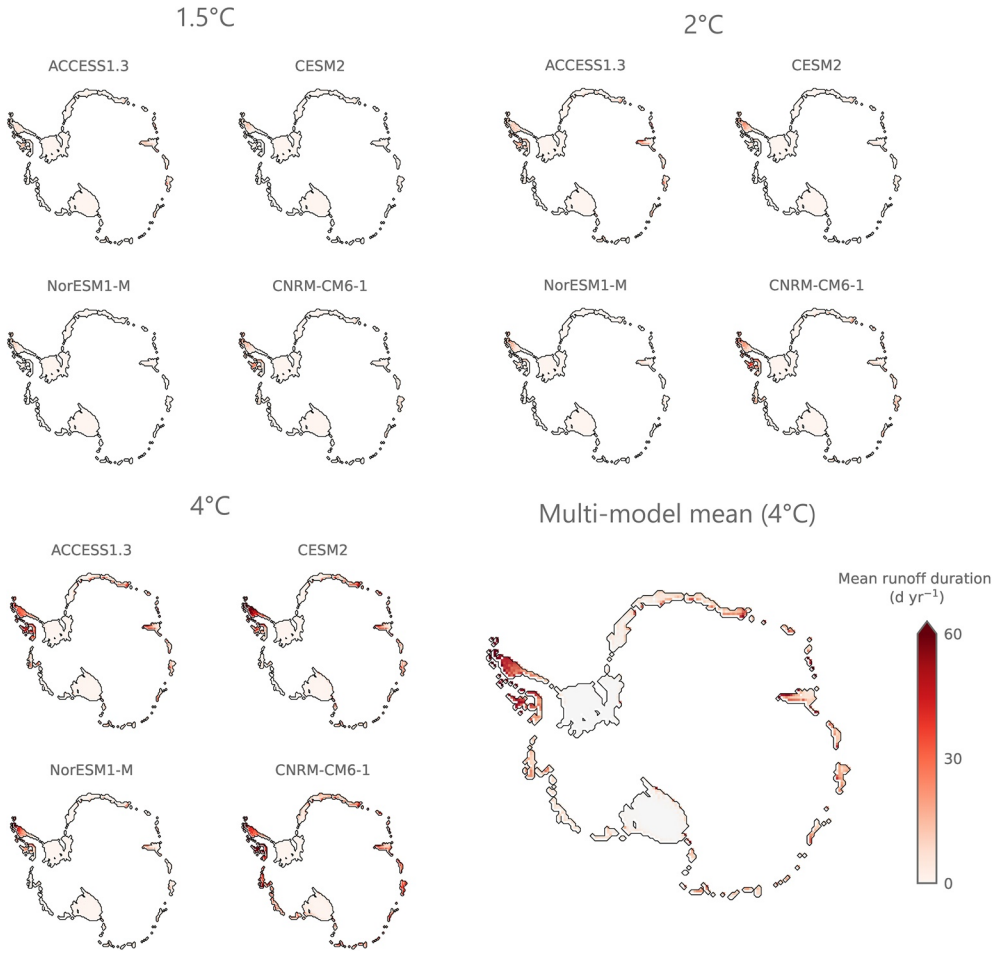

Figure 4. Mean number of days per year when runoff exceeding 1 kg m^{-2} d^{-1} is simulated by MAR forced with each GCM in the 1.5°C, 2°C, and 4°C scenarios, and the multi-model mean runoff duration simulated under the 4°C scenario. GCM, global climate models; MAR, Modèle Atmosphérique Régional.

yr^{-1} (1–8 d yr^{-1}) at 4°C (Figure 4). At 4°C, the maximum MMM number of days where liquid is simulated at the surface is 34 on the Pine Island ice shelf, although this rises to 69 d y^{-1} on the Abbot ice shelf in CNRM-CM6-1.

In East Antarctica, surface liquid water is confined to specific locations near the grounding lines of ice shelves representing 14.1% (10.0%–32.7%) of total area at 1.5°C and 58.2% (33.9%–69.7%) at 4°C (Figure 3). Specifically, at 4°C surface liquid water is present on parts of the Shackleton, Amery, West, and King Baudoin ice shelves, with the largest and smallest spatial extent in CNRM-CM6-1 and NorESM1-M, respectively. Averaged across all East Antarctic ice shelves, runoff is simulated during 2 d yr^{-1} (1–3 d yr^{-1}) at 1.5°C and 10 (4–12 d yr^{-1}) at 4°C. In all simulations, runoff extent and duration are highest on the Amery, King Baudoin and Shackleton ice shelves, where MMM runoff occurs up to 83, 81 and 71 d yr^{-1}, respectively 4°C (Figures 4 and S8).

2.3. Consequences for Sea Level Rise

Figures 3 and 4 show that warmer futures are associated with more intense and extensive runoff that increases the risk of hydrofracture-induced destabilization, especially if concentrated in areas that also provide buttressing. However, because this study does not consider ice and ocean dynamical drivers of ice shelf destabilization, this precludes a definitive prediction of which ice shelves are most likely to collapse. Of those ice shelves where considerable runoff is simulated (Figure 4), the dynamical stress regime on the

Amery, King Baudoin, and George VI shelves suggest they are resilient to hydrofracture (Lai et al., 2020). However, the Larsen C, Wilkins, Pine Island, and Shackleton ice shelves are identified as vulnerable by both Lai et al. (2020) and this study and so are considered most at-risk.

The use of an RCM adds greater detail to previous studies that used coarser resolutions and adds understanding of the processes that influence the destabilization of Antarctic ice shelves. Those we identify as vulnerable may be targeted for further work to understand their likely future and consequences for global sea level rise. However, our results are limited by using a single RCM, and future work should address this by using an ensemble of RCMs to downscale GCM projections. Although MAR is shown to under-estimate historical surface melt (Donat-Magnin et al., 2020; Kittel et al., 2021), its lack of a water-routing scheme means that runoff is likely over-estimated. In reality, meltwater can fill lakes above or below the surface or be transported laterally and exported to the ocean (Bell et al., 2018), reducing the likelihood of meltwater contributing to hydrofracturing. Therefore, our projections probably over-estimate the risk of melt- and runoff-induced destabilization.

Overall, the results suggest that elevated melt and runoff could contribute to the declining stability of a larger proportion of ice shelves in future, with consequent ramifications for sea level rise. In agreement with previous studies, the likelihood of hydrofracturing-induced collapse or mass loss is greatest on the Antarctic Peninsula, and to some extent the Pine Island and Shackleton ice shelves.

3. Conclusions

The warming scenarios examined represent plausible levels of warming for the 21st century. More warming results in increased melt, driving saturation of the snowpack and increasing runoff amount, duration and extent over ice shelves. These changes cause area-averaged SMB to decrease, although it remains positive, meaning Antarctic ice shelves will not directly contribute to sea level rise under the scenarios examined. Crucially however, the melt and runoff amounts simulated by MAR in all experiments indicate that ice shelves could be destabilized via hydrofracturing and thus contribute to sea level rise indirectly, especially if melt is concentrated in already-weak areas that buttress significant quantities of upstream ice. The extent of ice shelf mass loss and the precise fate of individual ice shelves depends primarily on the amount of warming that occurs. At 4°C above pre-industrial temperatures, 34% of all ice shelves (18%, 61%, and 67% for West Antarctica, East Antarctica and the Antarctic Peninsula, respectively) will experience annual mean runoff that suggests an increased risk of destabilization, including the Larsen C, Wilkins, Pine Island, and Shackleton ice shelves. At 1.5°C and 2°C however, the total ice shelf area vulnerable to collapse is reduced to 14%–18% (3%–5%, 21%–30%, and 46%–52% for West Antarctica, East Antarctica and the Antarctic Peninsula, respectively). The implication is that warming of 4°C above pre-industrial levels will almost quadruple the area vulnerable to hydrofracturing and hence probably increase the likelihood of ice shelf disintegration.

Conflicts of Interest

The authors declare no conflicts of interest.

Data Availability Statement

MAR output are archived by forcing GCM at: 10.5281/zenodo.4525735 (ACCESS1.3); 10.5281/zenodo.4528998 (NorESM1-M); 10.5281/zenodo.4529002 (CESM2); and 10.5281/zenodo.4529004 (CNRM-CM6-1). Forcing GCM data are available via the Earth System Grid Federation (https://esgf.llnl.gov/). Code used for analysis are available at 10.5281/zenodo.4543706.

Acknowledgments
The authors thank Andrew Orr and Charles Amory for helpful comments received during the preparation of this manuscript, as well as Brooke Medley and another anonymous reviewer. Computational resources for MAR simulations were provided by the Consortium des Équipements de Calcul Intensif (CÉCI), funded by the Fonds de la Recherche Scientifique de Belgique (FNRS) under grant no. 2.5020.11 and the Tier-1 supercomputer (Zenobe) of the Fédération Wallonie Bruxelles infrastructure funded by the Walloon Region under grant agreement no. 1117545. CK's work was supported by the FNRS under grant no. T.0002.16 and EG acknowledges funding from the British Antarctic Survey Innovation Voucher fund.

References

Agosta, C., Amory, C., Kittel, C., Orsi, A., Favier, V., Gallée, H., et al. (2019). Estimation of the Antarctic surface mass balance using the regional climate model MAR (1979–2015) and identification of dominant processes. *The Cryosphere*, *13*, 281–296. https://doi.org/10.5194/tc-13-281-2019

Agosta, C., Fettweis, X., & Datta, R. (2015). Evaluation of the CMIP5 models in the aim of regional modelling of the Antarctic surface mass balance. *The Cryosphere*, *9*, 2311–2321. http://doi.org/10.5194/tc-9-2311-2015

Bell, R. E., Banwell, A. F., Trusel, L. D., & Kingslake, J. (2018). Antarctic surface hydrology and impacts on ice-sheet mass balance. *Nature Climate Change*, *8*(December), 1044–1052. https://doi.org/10.1038/s41558-018-0326-3

Borstad, C. P., Rignot, E., Mouginot, J., & Schodlok, M. P. (2013). Creep deformation and buttressing capacity of damaged ice shelves: Theory and application to Larsen C ice shelf. *The Cryosphere*, *7*(6), 1931–1947. https://doi.org/10.5194/tc-7-1931-2013

Donat-Magnin, M., Jourdain, N. C., Gallée, H., Amory, C., Kittel, C., Fettweis, X., et al. (2020). Interannual variability of summer surface mass balance and surface melting in the Amundsen sector, West Antarctica. *The Cryosphere*, *14*(1), 229–249. https://doi.org/10.5194/tc-14-229-2020

Donat-Magnin, M., Jourdain, N. C., Kittel, C., Agosta, C., Amory, C., Gallée, H., et al. (2021). Future surface mass balance and surface melt in the Amundsen sector of the West Antarctic Ice Sheet. *The Cryosphere*, *15*, 571–593. https://doi.org/10.5194/tc-2020-113

Favier, V., Krinner, G., Amory, C., Gallée, H., Beaumet, J., & Agosta, C. (2017). Antarctica-regional climate and surface mass budget. *Current Climate Change Reports*, *3*(4), 303–315. https://doi.org/10.1007/s40641-017-0072-z

Fürst, J. J., Durand, G., Gillet-chaulet, F., Tavard, L., Rankl, M., Braun, M., & Gagliardini, O. (2016). The safety band of Antarctic ice shelves. *Nature Climate Change*, *6*(5), 479–482. https://doi.org/10.1038/NCLIMATE2912

Gallée, H. (1995). Simulation of the mesocyclonic activity in the Ross Sea, Antarctica. *Monthly Weather Review*, *123*(7), 205–2069. https://doi.org/10.1175/1520-0493(1995)123<2051:SOTMAI>2.0.CO;2

Gallée, H., & Duynkerke, P. G. (1997). Air-snow interactions and the surface energy and mass balance over the melting zone of west Greenland during the Greenland Ice Margin Experiment. *Journal of Geophysical Research*, *102*(D12), 13813–13824. https://doi.org/10.1029/96JD03358

Gallée, H., & Gorodetskaya, I. V. (2010). Validation of a limited area model over Dome C, Antarctic Plateau, during winter. *Climate Dynamics*, *34*(1), 61. https://doi.org/10.1007/s00382-008-0499-y

Gallée, H., Guyomarc'h, G., & Brun, E. (2001). Impact of snow drift on the Antarctic ice sheet surface mass balance: Possible sensitivity to snow-surface properties. *Boundary-Layer Meteorology*, *99*(1), 1–19. https://doi.org/10.1023/A:1018776422809

Gallée, H., & Schayes, G. (1994). Development of a three-dimensional meso-γ primitive equation model: Katabatic winds simulation in the area of Terra Nova Bay, Antarctica. *Monthly Weather Review*, *122*, 671–685. https://doi.org/10.1175/1520-0493(1994)122%3C0671:DOATDM%3E2.0.CO;2

Gudmundsson, G. H., Paolo, F. S., Adusumilli, S., & Fricker, H. A. (2019). Instantaneous Antarctic ice sheet mass loss driven by thinning ice shelves. *Geophysical Research Letters*, *46*(23), 13903–13909. https://doi.org/10.1029/2019GL085027

Hawkins, E., & Sutton, R. (2011). The potential to narrow uncertainty in projections of regional precipitation change. *Climate Dynamics*, *37*(1), 407–418. https://doi.org/10.1007/s00382-010-0810-6

Kingslake, J., Ely, J. C., Das, I., & Bell, R. E. (2017). Widespread movement of meltwater onto and across Antarctic ice shelves. *Nature*, *544*(7650), 349–352. https://doi.org/10.1038/nature22049

Kittel, C., Amory, C., Agosta, C., Jourdain, N. C., Hofer, S., Doutreloup, S., et al. (2021). Diverging surface mass balance projections between the Antarctic ice shelves and grounded ice sheet in 2100. *The Cryosphere*, *15*(3), 1215–1236. https://doi.org/10.5194/tc-2020-291

Kuipers Munneke, P., Ligtenberg, S. R. M., Van Den Broeke, M. R., & Vaughan, D. G. (2014). Firn air depletion as a precursor of Antarctic ice-shelf collapse. *Journal of Glaciology*, *60*(220), 205–214. https://doi.org/10.3189/2014JoG13J183

Kuipers Munneke, P., Luckman, A. J., Bevan, S. L., Smeets, C. J. P. P., Gilbert, E., Van Den Broeke, M. R., et al. (2018). Intense winter surface melt on an Antarctic ice shelf. *Geophysical Research Letters*, *45*, 7615–7623. https://doi.org/10.1029/2018GL077899

Lai, C.-Y., Kingslake, J., Wearing, M. G., Chen, P.-H. C., Gentine, P., Li, H., et al. (2020). Vulnerability of Antarctica's ice shelves to meltwater-driven fracture. *Nature*, *584*(7822), 574–578. https://doi.org/10.1038/s41586-020-2627-8

Lenaerts, J. T. M., Medley, B., Broeke, M. R., & Wouters, B. (2019). Observing and modeling ice sheet surface mass balance. *Reviews of Geophysics*, *57*(2), 376–420. https://doi.org/10.1029/2018rg000622

Lenaerts, J. T. M., Vizcaino, M., Fyke, J., van Kampenhout, L., & van den Broeke, M. R. (2016). Present-day and future Antarctic ice sheet climate and surface mass balance in the community earth system model. *Climate Dynamics*, *47*(5–6), 1367–1381. https://doi.org/10.1007/s00382-015-2907-4

Lhermitte, S., Sun, S., Shuman, C., Wouters, B., Pattyn, F., Wuite, J., et al. (2020). Damage accelerates ice shelf instability and mass loss in Amundsen Sea Embayment. *Proceedings of the National Academy of Sciences of the United States of America*, *117*(40), 24735–24741. https://doi.org/10.1073/pnas.1912890117

Ligtenberg, S. R. M., van de Berg, W. J., van den Broeke, M. R., Rae, J. G. L., & van Meijgaard, E. (2013). Future surface mass balance of the Antarctic ice sheet and its influence on sea level change, simulated by a regional atmospheric climate model. *Climate Dynamics*, *41*(3–4), 867–884. https://doi.org/10.1007/s00382-013-1749-1

Mottram, R., Hansen, N., Kittel, C., Van Wessem, M., Agosta, C., Amory, C., et al. (2021). What is the surface mass balance of Antarctica? An intercomparison of regional climate model estimates. *The Cryosphere*, 1–42. https://doi.org/10.5194/tc-2019-333

Paolo, F. S., Fricker, H. A., & Padman, L. (2015). Volume loss from Antarctic ice shelves is accelerating. *Science*, *348*(6232), 327–331. https://doi.org/10.1126/science.aaa0940

Pfeffer, W. T., Meier, M. F., & Illangasekare, T. H. (1991). Retention of Greenland runoff by refreezing: Implications for projected future sea level change. *Journal of Geophysical Research*, *96*(C12). https://doi.org/10.1029/91jc02502

Pritchard, H. D., Ligtenberg, S. R. M., Fricker, H. A., Vaughan, D. G., Van Den Broeke, M. R., & Padman, L. (2012). Antarctic ice-sheet loss driven by basal melting of ice shelves. *Nature*, *484*, 501–505. https://doi.org/10.1038/nature10968

Rignot, E., Casassa, G., Gogineni, P., Krabill, W., Rivera, A., & Thomas, R. (2004). Accelerated ice discharge from the Antarctic Peninsula following the collapse of Larsen B ice shelf. *Geophysical Research Letters*, *31*(18), 2–5. https://doi.org/10.1029/2004GL020697

Scambos, T. A., Hulbe, C., & Fahnestock, M. (2003). Climate-induced ice shelf disintegration in the Antarctic Peninsula. In E. Domack, A. Levente, A. Burnet, R. Bindschadler, P. Convey, & M. Kirby (Eds.), *Antarctic peninsula climate variability: Historical and paleoenvironmental perspectives* (Vol. 79, pp. 79–92). American Geophysical Union. https://doi.org/10.1029/AR079p0079

Scambos, T. A., Hulbe, C., Fahnestock, M., & Bohlander, J. (2000). The link between climate warming and break-up of ice shelves in the Antarctic Peninsula. *Journal of Glaciology*, *46*(154), 516–530. http://dx.doi.org/10.3189/172756500781833043

Shepherd, A., Ivins, E., Rignot, E., Smith, B., Van Den Broeke, M., Velicogna, I., et al. (2018). Mass balance of the Antarctic Ice Sheet from 1992 to 2017. *Nature*, *558*, 219–222. https://doi.org/10.1038/s41586-018-0179-y

Souverijns, N., Gossart, A., Demuzere, M., Lenaerts, J. T. M., Medley, B., Gorodetskaya, I. V., et al. (2019). A new regional climate model for POLAR-CORDEX: Evaluation of a 30-year Hindcast with COSMO-CLM2 over Antarctica. *Journal of Geophysical Research: Atmospheres*, *124*(3), 1405–1427. https://doi.org/10.1029/2018JD028862

Tedesco, M., Doherty, S., Fettweis, X., Alexander, P., Jeyaratnam, J., & Stroeve, J. (2016). The darkening of the Greenland ice sheet: Trends, drivers, and projections (1981–2100). *The Cryosphere*, *10*, 477–496. https://doi.org/10.5194/tc-10-477-2016

Trusel, L. D., Frey, K. E., Das, S. B., Karnauskas, K. B., Kuipers Munneke, P., van Meijgaard, E., & van den Broeke, M. R. (2015). Divergent trajectories of Antarctic surface melt under two twenty-first-century climate scenarios. *Nature Geoscience*, *8*(12), 927–932. https://doi.org/10.1038/ngeo2563

van den Broeke, M. R. (2005). Strong surface melting preceded collapse of Antarctic Peninsula ice shelf. *Geophysical Research Letters*, *32*, 2–5. https://doi.org/10.1029/2005GL023247

van Wessem, J. M., van de Berg, W. J., Noël, B. P. Y., van Meijgaard, E., Amory, C., Birnbaum, G., et al. (2018). Modelling the climate and surface mass balance of polar ice sheets using RACMO2–Part 2: Antarctica (1979–2016). *The Cryosphere*, *12*, 1479–1498. https://doi.org/10.5194/tc-2017-202

References From the Supporting Information

Barthel, A., Agosta, C., Little, C. M., Hattermann, T., Jourdain, N. C., Goelzer, H., et al. (2020). CMIP5 model selection for ISMIP6 ice sheet model forcing: Greenland and Antarctica. *The Cryosphere*, *14*(3), 855–879. https://doi.org/10.5194/tc-14-855-2020

Datta, R. T., Tedesco, M., Agosta, C., Fettweis, X., Kuipers Munneke, P., & Van Den Broeke, M. R. (2018). Melting over the northeast Antarctic peninsula (1999–2009): Evaluation of a high-resolution regional climate model. *The Cryosphere*, *12*(9), 2901–2922. https://doi.org/10.5194/tc-12-2901-2018

De Ridder, K., & Gallée, H. (1998). Land surface-induced regional climate change in southern Israel. *Journal of applied meteorology*, *37*(11), 1470–1485. https://doi.org/10.1175/1520-0450(1998)037<1470:LSIRCC>2.0.CO;2

Gallée, H., & Gorodetskaya, I. V. (2008). Validation of a limited area model over Dome C, Antarctic Plateau, during winter. *Climate Dynamics*, *34*(1), 61–72. https://doi.org/10.1007/s00382-008-0499-y

Gettelman, A., Hannay, C., Bacmeister, J. T., Neale, R. B., Pendergrass, A. G., Danabasoglu, G., et al. (2019). High climate sensitivity in the community earth system model version 2 (CESM2). *Geophysical Research Letters*, *46*(14), 8329–8337. https://doi.org/10.1029/2019GL083978

Iversen, T., Bentsen, M., Bethke, I., Debernard, J. B., Kirkevåg, A., Seland, Ø., et al. (2013). The Norwegian earth system model, NorESM1-M—Part 2: Climate response and scenario projections. *Geoscientific Model Development*, *6*(2), 389–415. https://doi.org/10.5194/gmd-6-389-2013

Meehl, G. A., Senior, C. A., Eyring, V., Flato, G., Lamarque, J. F., Stouffer, R. J., et al. (2020). Context for interpreting equilibrium climate sensitivity and transient climate response from the CMIP6 Earth system models. *Science Advances*, *6*(26), 1–11. https://doi.org/10.1126/sciadv.aba1981

Palerme, C., Genthon, C., Claud, C., Kay, J. E., Wood, N. B., & L'Ecuyer, T. (2017). Evaluation of current and projected Antarctic precipitation in CMIP5 models. *Climate Dynamics*, *48*, 225–239. https://doi.org/10.1007/s00382-016-3071-1

Voldoire, A., Saint-Martin, D., Sénési, S., Decharme, B., Alias, A., Chevallier, M., et al. (2019). Evaluation of CMIP6 DECK experiments with CNRM-CM6-1. *Journal of Advances in Modeling Earth Systems*, *11*(7), 2177–2213. https://doi.org/10.1029/2019MS001683